



Cite this: *RSC Adv.*, 2020, **10**, 6654

Received 19th December 2019
 Accepted 3rd February 2020

DOI: 10.1039/d0ra00601g
rsc.li/rsc-advances

Functionalized natural cellulose fibres for the recovery of uranium from seawater†

Adrian Tellería-Narvaez, Whitney Talavera-Ramos, Lucas Dos Santos, Jimena Arias, Alejandro Kinbaum and Vittorio Luca*

Sisal fibres have been functionalized with aminotrimethylenephosphonic acid (ATMP) and *N*-(phosphonomethyl)glycine (glyphosate) by hydrothermal reaction in dilute solutions of the phosphonates at temperatures in the range 120–180 °C. The hydrothermal treatment results in delignification and anchoring of the phosphonate. The functionalized fibers show greatly enhanced efficiency for the recovery of uranium from seawater relative to the untreated fibres and possess capacities up to 16 mg g⁻¹ in spiked seawater and relatively rapid kinetics reaching a maximum uptake in under 1 h.

Nuclear fission is a dense form of energy generation that is generally considered to produce few carbon emissions especially if the uranium utilized derives from high grade ore.¹ It has been suggested that a significant build-out of fission nuclear energy would represent an effective measure to combat climate change.²

A sustainable expansion of low carbon-emitting nuclear fission energy based on the ²³⁸U–²³⁹Pu fuel cycle would require a plentiful supply of high-grade uranium ore the availability of which is already limited.

Considering that the world's oceans contain about 4 billion tonnes of uranium at a concentration of about 3–4 ppb predominantly in the form of the UO₂(CO₃)₃⁴⁻ ion, seawater represents a potentially limitless uranium resource if it can be recovered economically.

A variety of separation technologies have been explored for uranium recovery from seawater including nanofiltration membranes,^{3,4} nanostructured metal oxides,⁵ biomass,^{6,7} biopolymers, micro-organisms⁸ and synthetic polymers. Most recently electrolytic processes have also been proposed.⁹

As ostensibly attractive as adsorption technologies are, each material class has its advantages and disadvantages.¹⁰ Of the synthetic polymers, amidoxime fibres have garnered by far the most interest as they offer a powerful combination of materials properties including selectivity, capacity and stability in marine conditions. Amidoxime-functionalized polymers have been studied since the early eighties¹¹ and can be deployed at small scale in fluidized beds¹² and in granular and fibrous forms.^{13,14} Gram-scale production of UO₂ has been demonstrated in

floating pontoons that support submerged cages containing weaves.¹⁵

Recently a new generation of amidoxime fibres with high capacity have been reported using Atom-Transfer Radical Polymerization (ATRP) from poly(vinyl chloride)-*co*-chlorinated poly(vinyl chloride) (PVC-*co*-CPVC)¹⁶ and high surface area amidoxime-based polymer fibres co-grafted with various acids.¹⁷ However, phosphonic acid-functionalized polymers prepared by radiation-induced grafting techniques have also been of interest for some time.^{18,19}

Das *et al.*²⁰ reported the use polymers prepared by the Radiation-Induced Graft Polymerization (RIGP) of acrylonitrile (AN) and vinylphosphonic acid (VPA) as well as carboxylate functionalized polymers using AN and itaconic acid.²¹ Such fibres, as well as those prepared by atom-transfer polymerization, are unlikely to be inexpensive considering the cost of precursors and the number of synthetic steps involved.¹⁶ The latest generation of graft polymers prepared by either ATRP or RIGP have maximum capacity for uranium in the range 4–5 mg g⁻¹ measured in spiked seawater.²² New generation fibres having amidoxime functionality attached to sophisticated high surface area substrates have now reached capacities in excess of 1000 mg U g⁻¹ in spiked seawater and 10 mg U g⁻¹ in natural seawater.^{23–25}

Compared to petrochemical-based polymers, natural fibres such as Sisal and Hemp can be mass produced, are likely to have a significant cost advantage, and most importantly, they are renewable materials. Methods for improving the surface properties of cellulose-based renewable materials involving radiation-induced grafting and direct functionalization have been extensively explored.²⁶

In the present communication we report on the functionalization of common Sisal fibres using a simple one-step hydrothermal process utilizing aminotrimethylenephosphonic (ATMP) acid and *N*-(phosphonomethyl)glycine as the uranium

Comisión Nacional de Energía Atómica, Av. General Paz 1499, 1650 San Martín, Buenos Aires, Argentina. E-mail: vluca@cnea.gov.ar; Tel: +54 11 6772 7018

† Electronic supplementary information (ESI) available. See DOI: [10.1039/d0ra00601g](https://doi.org/10.1039/d0ra00601g)



selective functional molecule. The latter is most commonly known as the herbicide glyphosate (GLY). Sisal is one of a number of renewable and inexpensive lignocellulosic fibres that have been in widespread use for more than century with current worldwide production of about 375 000 tonnes. ATMP and GLY were chosen for functionalization because they are also inexpensive and due to the well-known affinity that phosphonates and carboxylates have for actinide elements, and the ability of phosphonate groups to graft to hydroxylated surfaces as well as their cost effectiveness. The present functionalization method is extremely simple relative to previously reported methods²⁶ and yields materials with excellent efficiency for the recovery of uranium from seawater.

Commonly available Sisal twine was utilized in this work. The two phosphonic acids ATMP and GLY with structures as shown below were supplied by Sigma-Aldrich and Gleba S. A. respectively. See ESI† section for the molecular structures.

The functionalization procedure involved hydrothermal treatment of the fibres in dilute solutions of the phosphonate at various temperatures. See ESI† section for synthetic details. The products are referred to as ATMP-Sisal-*x* and GLY-Sisal-*x* where *x* is the hydrothermal treatment temperature.

Phosphorus was never observed in any of the seawater supernatants indicating that the phosphonic acids were firmly anchored under the given conditions.

X-ray diffraction patterns comparing ATMP-Sisal-150 and GLY-Sisal-150 with unreacted Sisal fibres are shown in Fig. 1a–c. Following hydrothermal treatment with GLY and ATMP the linewidth (FWHM) of the (002) reflection of cellulose shows a dramatic decrease from 3.22 to 1.85 and 2.17° 2θ for ATMP-Sisal-150 and GLY-Sisal-150 respectively indicating an improvement in the crystalline ordering of the cellulose matrix. The crystallinity index for all three samples falls in the range 70–90%.

The FTIR spectrum of the untreated Sisal (Fig. 1d) is typical of that reported in the literature.²⁸ Functionalization with either phosphonate (Fig. 1e and f) results in the elimination of the intense 1250 cm⁻¹ band assigned to δ(C-OH) vibrations of the glucosidic rings²⁸ and the appearance of a weak band at 1204 cm⁻¹ consistent with vibrations of the -PO(OH)₂ group. Additionally, it can be observed that the intensity of the ν(C=O) ester vibration (1720 cm⁻¹) is being reduced and a new ester band arises at 1710 cm⁻¹. The intensity of the former band is reduced proportionately with the P content of the fibres (Fig. S2†). These changes are consistent with grafting of the phosphonates and are supported by the fact that P cannot be detected in solution after the sorption experiments.

SAXS measurements of the unfunctionalized and functionalized fibres showed Porod law behaviour in the high *q* region indicating a sharp phase boundary for both samples. Large differences were observed in the Porod constant after hydrothermal reactions consistent with sharpening of this boundary (Fig. S3†).

The degree of uranium recovery from the 4 ppm spiked seawater by the variously treated Sisal fibres is shown in Fig. 2.

Untreated sisal fibres that had been treated hydrothermally in water or water–ethanol solutions for the same period of time

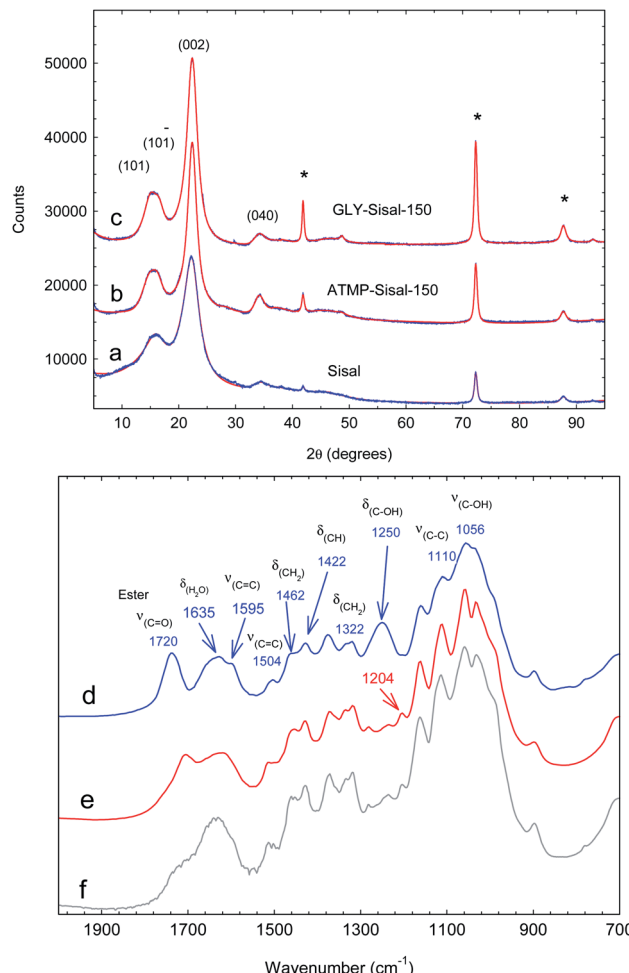


Fig. 1 (a–c) XRD powder patterns of ground Sisal and functionalized Sisal fibres. Patterns have been fitted using the methodology of Ju *et al.*²⁷ The reflections marked by * are due to the support. (d–f) FTIR spectra of untreated Sisal fibres, ATMP-Sisal-150 and GLY-Sisal-150 respectively.

as the samples treated with phosphonate solution did not sorb uranium from the 4 ppm U seawater solution. Hydrothermal treatment of Sisal fibres with deionized water resulted in increasing extraction of uranium as a function of temperature reaching 50% for W-Sisal-180. Hydrothermal treatment in the water–ethanol mixture was relatively ineffective at increasing extraction efficiency over the entire temperature range. The extraction efficiency of the ATMP-Sisal-150 was quantitative while the GLY-Sisal-150 fibres extracted about 90% of the uranium. The GLY-Sisal-180 fibres extracted uranium quantitatively.

Sisal fibres treated hydrothermally at 150 °C in 0.1 M solutions of H₂SO₄ and H₃PO₄ were also tested using the same protocol. Uranium uptake on these acid-treated fibres never exceeded 30–50% for these materials confirming that the enhanced performance is due to phosphonate functionalization. The materials show strong sorption of uranium in the pH range 3–9 (Fig. S4†) but little adsorption below about 2 suggesting that sorbed uranium could be easily eluted.



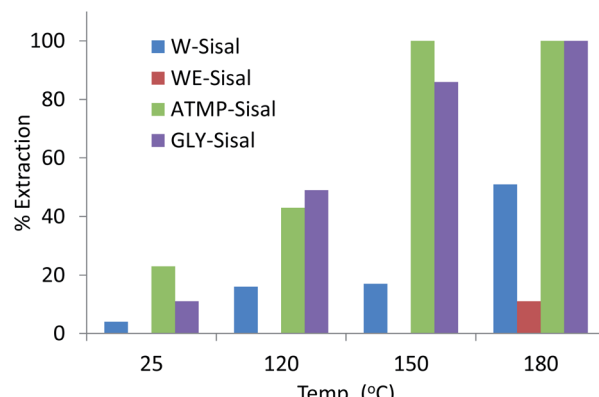


Fig. 2 Uranium uptake by Sisal fibres treated hydrothermally with different phosphonate solutions at increasing temperature. Initial U concentration of seawater used was 4.0 ppm.

A rough measure of the sorption capacity of the phosphonate-functionalized fibres to extract uranium from seawater was obtained using a 10 ppm uranium seawater solution and volume/mass (v/m) ratios of between 300 and 3000 mL g^{-1} . These results all indicated a saturation capacity in the range 2–3 mg U g^{-1} .

Detailed measurements of the sorption isotherms were performed for ATMP-Sisal-150 and GLY-Sisal-150 using the spiked 10 ppm U seawater solution and varying the v/m ratio (Fig. S5†). Langmuir fits of these data gave capacities of 3.2 and 2.3 mg g^{-1} for ATMP-Sisal-150 and GLY-Sisal-150 respectively. These capacity values are not substantially lower than the best performing synthetic amidoxime polymers reported until 2017 that have capacity values in the range 4–5 mg g^{-1} .²² We have observed however that simply increasing the phosphonate solution concentration during functionalization can yield materials having capacities as high as 16 mg g^{-1} in spiked seawater (10 ppm). In natural seawater we have obtained values of capacity of the order of 0.1 mg g^{-1} .

The kinetics of adsorption of the best performing materials were measured (Fig. 3a) and show that maximum adsorption is achieved within the first hour for both materials for U feed concentrations of a few ppm. These are relatively slow kinetics for an adsorbent material but are fast compared with synthetic amidoxime fibres that typically take around 20 days to reach maximum uptake.

Although the extraction of U from seawater would not employ fixed-bed columns, the testing of the functionalized fibres under dynamic conditions in fixed bed columns is relevant to other applications. Therefore column breakthrough curves were measured for the functionalized Sisal fibres and a typical curve is presented for GLY-Sisal-150 (Fig. 3b). Breakthrough was observed after reaching a loading of about 0.15 mg U g^{-1} sorbent. The early breakthrough and slow decline in the C/C_0 value beyond the peak is probably due to the residence time being relatively short compared to the adsorption kinetics of the functionalized Sisal and the fact that column packing was not optimized. Since as previously mentioned U sorption falls off dramatically at low pH, elution with strong and weak acids is possible (Fig. S4†). Both

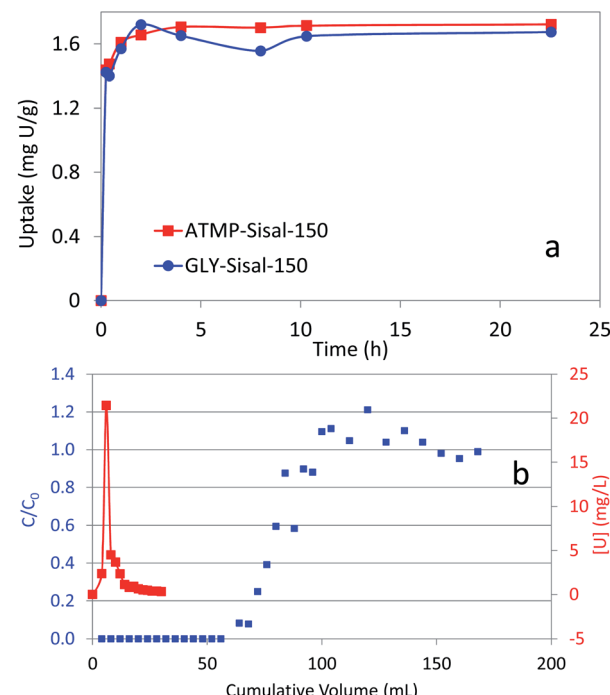


Fig. 3 (a) Sorption kinetics of ATMP-Sisal-150 (■) and GLY-Sisal-150 (●). $[\text{U}]_{\text{initial}} = 5.9 \text{ mg L}^{-1}$, $v/m = 200 \text{ mL g}^{-1}$ (b) column breakthrough and elution (0.20 M citric acid) curve for GLY-Sisal-150 loaded column. Column volume = 3.4 mL, flow rate = 0.20 mL min^{-1} .

HCl (1 M) and citric acid (0.20 M, pH 2.0) were tested and were shown to be effective in eluting uranium from the both GLY-Sisal-150 and ATMP-Sisal-150. The use of 1.0 M HCl appeared to be particularly efficient with the bulk of the U being eluted in only 15 mL of eluent (Fig. 3b). Multiple loading and elution of the column was also found to be possible.

This work has demonstrated that an exceedingly simple hydrothermal treatment of extremely cost-effect Sisal twine with similarly inexpensive relatively dilute phosphonic acid solutions results in delignification and functionalization of the fibres. Phosphonate functionalization results in a substantial increase in the capacity of the Sisal fibres to sorb uranium from seawater. Of the two phosphonic acids investigated hydrothermal reaction above 120 °C using dilute ATMP solution consistently resulted in materials with slightly superior capacity at the expense of fibre cleavage.

It is hypothesized that both phosphonic acids become grafted to the fibres through condensation reactions between the phosphonate groups and hydroxyl groups of the cellulose. Similar reactions are observed between organophosphonates and the hydroxylated surfaces of group (IV) metal oxides^{29,30} and layered double hydroxides (LDH). The thermal and hydrothermal stability of glyphosate grafted to the hydroxyl surfaces of LDH has been demonstrated at temperatures in excess of 180 °C.³¹ If it is the phosphonate group that grafts to the cellulose surface then it must be the carboxylate groups of the glyphosate that bind uranium. In support of this hypothesis we have observed that commercial aminodcarboxylate resins can also extract uranium efficiently from seawater at the



concentrations investigated in this study. However, these materials certainly cannot compete with the present materials. The present one-step functionalization is extremely simple to implement compared to more sophisticated multi-step methods reported in the literature such as the classical TEMPO-mediated oxidation.

This preliminary work opens the way to a potentially new and vast class of renewable and extremely cost-effective materials for applications to uranium recovery from seawater provided capacity can be significantly optimized. The materials could also have applications in the decontamination of surface and ground waters as well as the efficient extraction of other heavy metals.

Conflicts of interest

There are no conflicts to declare.

Notes and references

- 1 E. S. Warner and G. A. Heath, *J. Ind. Ecol.*, 2012, **16**, S73.
- 2 J. Hansen, M. Sato, P. Kharecha, K. von Schuckmann, D. J. Beerling, J. Cao, S. Marcott, V. Masson-Delmotte, M. J. Prather, E. J. Rohling, J. Shakun, P. Smith, A. Lacis, G. Russell and R. Ruedy, *Earth Syst. Dynam.*, 2017, **8**, 577.
- 3 A. Favre-Reguillon, G. Lebuzit, J. Foos, A. Guy, A. Sorin, M. Lemaire and M. Draye, *Sep. Sci. Technol.*, 2005, **40**, 623.
- 4 A. Favre-Reguillon, G. Lebuzit, J. Foos, A. Guy, M. Draye and M. Lemaire, *Ind. Eng. Chem. Res.*, 2003, **42**, 5900.
- 5 W. Chouyyok, C. L. Warner, K. E. Mackie, M. G. Warner, G. A. Gill and R. S. Addleman, *Ind. Eng. Chem. Res.*, 2016, **55**, 4195.
- 6 M. Fujii, S. Shioya and A. Ito, *Holzforschung*, 1988, **42**, 295.
- 7 Z. Bai, Q. Liu, H. Zhang, J. Liu, J. Yu and J. Wang, *Chem. Eng. J.*, 2020, **382**, 122555.
- 8 T. Sakaguchi, T. Horikoshi and A. Nakajima, *J. Ferment. Technol.*, 1978, **56**, 561.
- 9 F. Chi, S. Zhang, J. Wen, J. Xiong and S. Hu, *Ind. Eng. Chem. Res.*, 2018, **57**, 8078.
- 10 J. Kim, C. Tsouris, R. T. Mayes, Y. Oyola, T. Saito, C. J. Janke, S. Dai, E. Schneider and D. Sachde, *Sep. Sci. Technol.*, 2013, **48**, 367.
- 11 L. Astheimer, H. J. Schenk, E. G. Witte and K. Schwochau, *Sep. Sci. Technol.*, 1983, **18**, 307.
- 12 M. Kanno, *J. Nucl. Sci. Technol.*, 1984, **21**, 1.
- 13 K. Sugasaka, S. Katoh, N. Takai, H. Takahashi and Y. Umezawa, *Sep. Sci. Technol.*, 1981, **16**, 971.
- 14 N. Kabay, A. Katakai, T. Sugo and H. Egawa, *J. Appl. Polym. Sci.*, 1993, **49**, 599.
- 15 N. Seko, A. Katakai, S. Hasegawa, M. Tamada, N. Kasai, H. Takeda, T. Sugo and K. Saito, *Nucl. Technol.*, 2003, **144**, 274.
- 16 S. Brown, Y. Yue, L.-J. Kuo, N. Mehio, M. Li, G. Gill, C. Tsouris, R. T. Mayes, T. Saito and S. Dai, *Ind. Eng. Chem. Res.*, 2016, **55**, 4139.
- 17 Y. Oyola, C. J. Janke and S. Dai, *Ind. Eng. Chem. Res.*, 2016, **55**, 4149.
- 18 H. Egawa, N. Kabay, A. Jyo, M. Hirono and T. Shuto, *Ind. Eng. Chem. Res.*, 1994, **33**, 657.
- 19 H. Egawa, N. Kabay, T. Shuto and A. Jyo, *Ind. Eng. Chem. Res.*, 1993, **32**, 540.
- 20 S. Das, Y. Oyola, R. T. Mayes, C. J. Janke, L.-J. Kuo, G. Gill, J. R. Wood and S. Dai, *Ind. Eng. Chem. Res.*, 2016, **55**, 4103.
- 21 S. Das, Y. Oyola, R. T. Mayes, C. J. Janke, L.-J. Kuo, G. Gill, J. R. Wood and S. Dai, *Ind. Eng. Chem. Res.*, 2016, **55**, 4110.
- 22 C. W. Abney, R. T. Mayes, T. Saito and S. Dai, *Chem. Rev.*, 2017, **117**, 13935.
- 23 Y. Yuan, S. Zhao, J. Wen, D. Wang, X. Guo, L. Xu, X. Wang and N. Wang, *Adv. Funct. Mater.*, 2019, **29**, 1805380.
- 24 X. Xu, H. Zhang, J. Ao, L. Xu, X. Liu, X. Guo, J. Li, L. Zhang, Q. Li, X. Zhao, B. Ye, D. Wang, F. Shen and H. Ma, *Energy Environ. Sci.*, 2019, **12**, 1979.
- 25 D. Wang, J. Song, S. Lin, J. Wen, C. Ma, Y. Yuan, M. Lei, X. Wang, N. Wang and H. Wu, *Adv. Funct. Mater.*, 2019, 1901009.
- 26 K. Bethke, S. Palantöken, V. Andrei, M. Rof, V. S. Raghuwanshi, F. Kettemann, K. Greis, T. T. K. Ingber, J. B. Stückrath, S. Valiyaveettil and K. Rademann, *Adv. Funct. Mater.*, 2018, **28**, 1800409.
- 27 X. Ju, M. Bowden, E. E. Brown and X. Zhang, *Carbohydr. Polym.*, 2015, **123**, 476.
- 28 P. Garside and P. Wyeth, *Stud. Conserv.*, 2003, **48**, 269.
- 29 G. Guerrero, P. H. Mutin and A. Vioux, *Chem. Mater.*, 2001, **13**, 4367.
- 30 C. S. Griffith, M. D. L. Reyes, N. Scales, J. V. Hanna and V. Luca, *ACS Appl. Mater. Interfaces*, 2010, **2**, 3436.
- 31 F. Li, L. Zhang, D. G. Evans, C. Forano and X. Duan, *Thermochim. Acta*, 2004, **424**, 15.

